

See discussions, stats, and author profiles for this publication at: <https://www.researchgate.net/publication/5433504>

# (Thermo)dynamic Role of Receptor Flexibility, Entropy, and Motional Correlation in Protein–Ligand Binding

ARTICLE *in* CHEMPHYSICHEM · MAY 2008

Impact Factor: 3.42 · DOI: 10.1002/cphc.200700857 · Source: PubMed

---

CITATIONS

37

---

READS

24

2 AUTHORS, INCLUDING:



[Riccardo Baron](#)

Baron Research Group, New York, United St...

63 PUBLICATIONS 2,266 CITATIONS

SEE PROFILE

# (Thermo)dynamic Role of Receptor Flexibility, Entropy, and Motional Correlation in Protein–Ligand Binding

Riccardo Baron<sup>\*[a]</sup> and J. Andrew McCammon<sup>[a, b]</sup>

*The binding of 2-amino-5-methylthiazole to the W191G cavity mutant of cytochrome c peroxidase is an ideal test case to investigate the entropic contribution to the binding free energy due to changes in receptor flexibility. The dynamic and thermodynamic role of receptor flexibility are studied by 50 ns-long explicit-solvent molecular dynamics simulations of three separate receptor ensembles: W191G binding a K<sup>+</sup> ion, W191G–2a5mt complex with a closed 190–195 gating loop, and apo with an open loop.*

*We employ a method recently proposed to estimate accurate absolute single-molecule configurational entropies and their differences for systems undergoing conformational transitions. We find that receptor flexibility plays a generally underestimated role in protein–ligand binding (thermo)dynamics and that changes of receptor motional correlation determine such large entropy contributions.*

## 1. Introduction

Understanding protein–ligand binding and characterizing the underlying (thermo)dynamics is the fundamental prerequisite to develop effective drug-design procedures and a major challenge in the multidisciplinary area of computational biochemistry.<sup>[1–8]</sup> The binding of 2-amino-5-methylthiazole (2a5mt) to the W191G cavity mutant of cytochrome c peroxidase from *E. coli* (W191G) has been characterized by X-ray crystallography<sup>[9–12]</sup> and isothermal titration calorimetry<sup>[12]</sup> experiments, as well as by computational techniques.<sup>[13,14]</sup> This system is an ideal test case to investigate the magnitude of the entropy penalty to the binding free energy due to changes in receptor flexibility. Ligand binding affects the flexibility of both the W191G cavity and 190–195 gating-loop regions,<sup>[10,14]</sup> which may induce full opening of the gating loop in the case of benzimidazole (bzi).<sup>[10]</sup> However, a number of X-ray structures<sup>[12]</sup> and molecular dynamics (MD) simulations<sup>[14]</sup> suggest that no major rearrangements occur in other regions of the W191G protein upon binding of small compounds.

The role of flexibility in (bio)molecular recognition and protein–ligand binding is twofold. First, upon binding (bio)molecules modify their molecular shape<sup>[1–7,14–17]</sup> and their underlying motion (conformational dynamics).<sup>[14–17]</sup> Second, this involves compensating enthalpy and entropy contributions to the free energy determined by the accessed configurational space (thermodynamics),<sup>[18–20]</sup> which are inherently difficult to correlate to specific molecular interactions, both from experiment<sup>[21–26]</sup> and computation.<sup>[27–39]</sup> Experiments capturing single-molecule<sup>[20,35]</sup> thermodynamics are notoriously difficult,<sup>[22,26,35]</sup> while reliable entropy calculations require non-standard computational resources.<sup>[29,36]</sup> Insight into ligand single-molecule configurational entropy changes upon protein binding has been reported in recent years.<sup>[31,34,38,40]</sup> Simplified approaches have also been applied with some success to ligands binding to rigid receptors.<sup>[41,42]</sup>

Herein we investigate the dynamic and thermodynamic role of receptor flexibility using 50 ns-long explicit-solvent MD simulations of three separate receptor ensembles: W191G binding a K<sup>+</sup> ion (**ref**), W191G–2a5mt complex (**bb**) with a closed 190–195 gating loop, and apo with an open loop (**open**); see Table 1. We employ a method recently proposed to correct anharmonicity and correlation effects; this supplies accurate absolute single-molecule configurational entropies and their differences also for systems undergoing conformational transitions.<sup>[36]</sup> Additionally, we investigate how molecular motions and their correlations determine entropy changes upon ligand-binding using a complete quasiharmonic analysis.<sup>[36]</sup> We find that receptor flexibility plays a generally underestimated role in protein–ligand binding (thermo)dynamics.

## 2. Results and Discussion

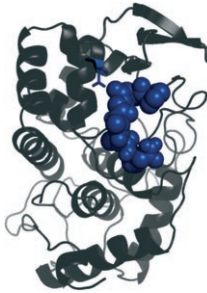
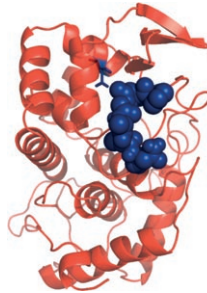
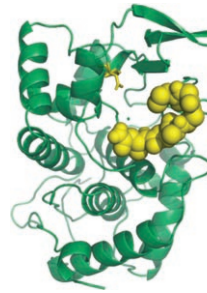
### 2.1. Receptor Dynamics and Flexibility

Figure 1 shows the conformational sampling of key side chains in the W191G cavity, their normalized probability distributions, and corresponding values from X-ray reference structures. We previously analyzed motional-averaging effects for the W191G system.<sup>[14]</sup> Longer 50 ns trajectories additionally reveal pronounced peaks for  $\chi$  of Lys 179 (around 90 deg; **open**) and

[a] Dr. R. Baron, Prof. Dr. J. A. McCammon  
Department of Chemistry & Biochemistry and  
Center for Theoretical and Biological Physics  
University of California at San Diego, La Jolla, CA 92093-0365 (USA)  
Fax: (+1) 858-534-4974  
E-mail: rbaron@mccammon.ucsd.edu

[b] Prof. Dr. J. A. McCammon  
Department of Pharmacology and  
Howard Hughes Medical Institute  
University of California at San Diego, La Jolla, CA 92093-0365 (USA)

**Table 1.** Molecular dynamics receptor ensembles characterized by different closed (blue) or open (yellow) binding and gating-loop states. Asp235 is also highlighted. The corresponding reference codes are used throughout the text. Sampling periods of 50 ns (after 5 ns pre-equilibration) at 300 K are employed for each system.

|                      |   |   |  |
|----------------------|---|---|--|
| MD receptor ensemble |  |  |  |
| Code                 | ref   | bb  | open   |
| Binding              | K <sup>+</sup>  | 2a5mt <sup>+</sup>  | apo  |
| Gating loop          | closed  | closed  | open   |
| Nr. solute atoms     | 3078  | 3089  | 3078   |
| Nr. water molecules  | 16826   | 16315   | 17030  |

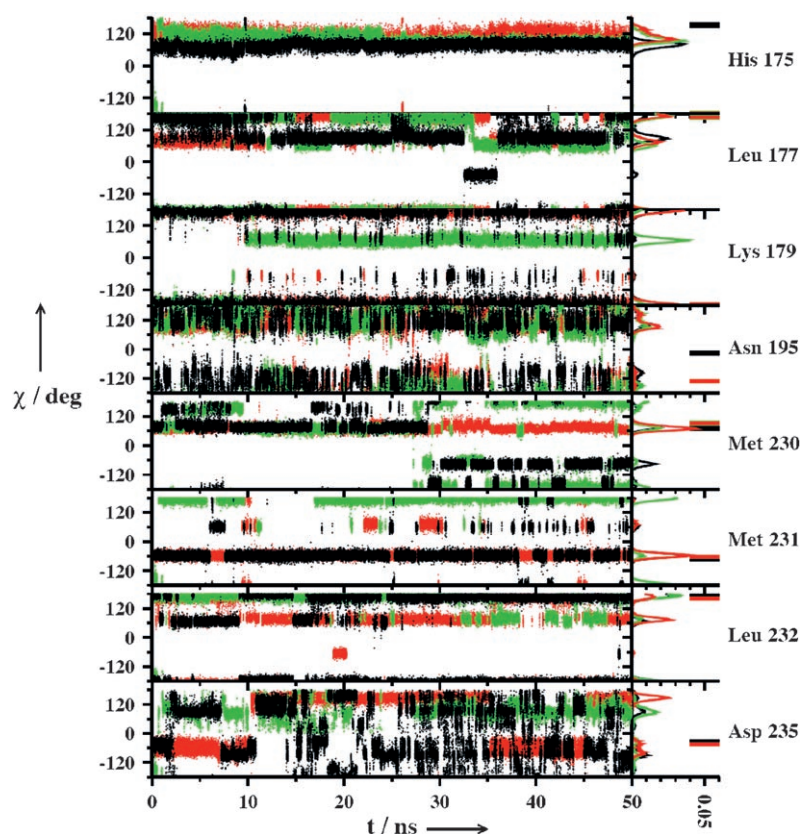


**Figure 1.** Torsional-angle  $\chi$  time series (left panels) and their normalized-probability distributions (right panels) characterizing the W191G cavity. The side-chain dihedral angles  $\chi$  ( $C^\alpha-C^\beta-X^\gamma-X^\delta$ , where X is a C, N, or O atom) are shown as calculated from **ref** (black), **bb** (red), and **open** (green) simulations. The horizontal lines (right panels) indicate the dihedral angles from corresponding X-ray crystallography structures. Units are  $\text{deg}^{-1}$  for distributions, horizontal axis. See Table 1 for reference codes.

Asp 235 (around 130 deg; **bb**). The side chains of Leu 177, Lys 179, Asn 195, Met 230, Met 231, and Asp 235 display comparatively narrower  $\chi$  dihedral angle distributions when 2a5mt binds the W191G cavity.

supporting previous suggestions concerning the slow kinetics of *cis-trans* isomerization for Pro 190.<sup>[10]</sup>

Dynamics and local flexibility are significantly perturbed upon binding of 2a5mt (**bb** vs **ref**) or upon opening of the gating loop and release of the K<sup>+</sup> ion from the cavity (**open** vs **ref**). As previously reported,<sup>[14]</sup> cavity hydration contributes to these alternative sampling behaviors. The timescales associated with  $\chi$  dihedral-angle transitions defining side-chain sampling inside the W191G cavity were also monitored (Supporting Information). For example, this analysis suggests that the Met 230 side chain is confined within one energy well when bound to 2a5mt, but experiences several dihedral transitions in **ref** and **open** simulations (see also Figure 1).

Figure 2 shows the time series of the atom-positional root-mean-square deviation (RMSD) for the gating-loop atoms of **ref**, **bb**, and **open** MD trajectory structures from alternatively the corresponding closed or open X-ray crystallography structures.<sup>[10,12]</sup> For simulations **ref** and **bb** RMSD values from the open X-ray reference structure (PDB ID: 1RYC) are significantly larger than those from the closed X-ray reference structures (PDB ID: 1AA4 and 1AEN, respectively). In contrast, the **open** trajectory structures remain closer to the open (PDB ID: 1RYC) than to the closed reference structure (PDB ID: 1AA4). In addition, we analyzed the conformational dynamics characterizing the loop-gating mechanism around its hinge points Pro 190 and Asn 195 (Figure S1). These results as a whole demonstrate that all simulations are characterized by closed-only or open-only loop configurations during the 50 ns periods, thus defining separate thermodynamic ensembles and

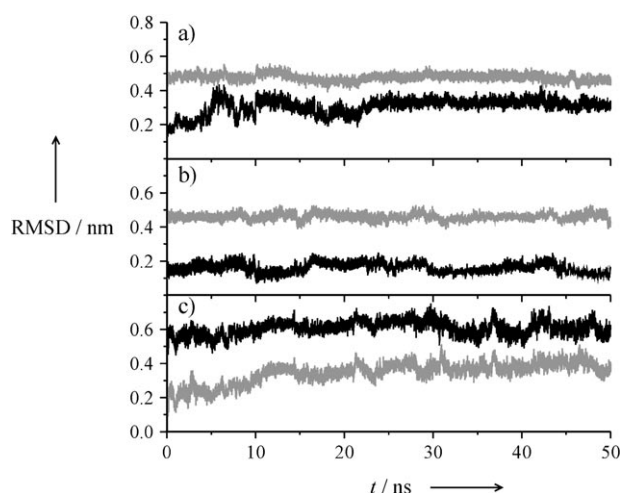


**Figure 2.** Time series of the backbone C $\alpha$  atom positional RMSD of the loop region of residues 190–195 of a) **ref**, b) **bb**, and c) **open** trajectory structures from corresponding closed-gate (black lines) and open-gate (gray lines) X-ray crystallography structures. Trajectory structures were superimposed using all backbone C $\alpha$  atoms of W191G.

## 2.2. Receptor Entropies, Anharmonicity, and Correlation

The convergence properties of the single-molecule quasiharmonic entropy  $S_{\text{qm}}^{\text{h}}$  as a function of the sampling time are illustrated in Figure 3, separately for the W191G cavity and gating-loop regions. All curves show stepwise buildup in the first 15–20 ns of the (pre-equilibrated) simulations. They level off within 30 ns for both the W191G cavity (Figure 3a) and the gating loop (Figure 3b) in **ref** and **bb** simulations. However, convergence requires at least 40 ns for the **open** simulation, and is faster for the cavity than the loop region. A large fraction of the configurational space of both regions can be sam-

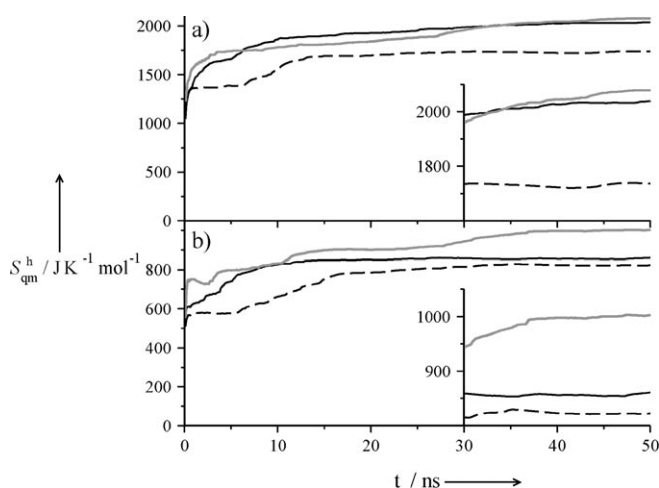


**Figure 3.** Convergence curves of the single-molecule quasiharmonic entropy upper bound  $S_{\text{qm}}^{\text{h}}$  for a) the W191G cavity and b) the 190–195 loop region as a function of sampling time for **ref** (black), **bb** (dashed black), and **open** (gray) simulations. The inset panels focus on the last 20 ns. To capture 99% of the final  $S_{\text{qm}}^{\text{h}}$  values (Table 2) 39 and 23, 23 and 29, 43 and 37 ns are required for the W191G cavity and the gating loop region of **ref**, **bb**, and **open** simulations, respectively. The numerical error in the final  $S_{\text{qm}}^{\text{h}}$  estimates is about 11 J K $^{-1}$  mol $^{-1}$  (see Computational Methods section).

pled within 20 ns when either 2a5mt or a K $^{+}$  cation binds to the W191G cavity.

Single-molecule energetic contributions, quasiharmonic entropies  $S_{\text{qm}}^{\text{h}}$  (calculated throughout the 50 ns simulations and including the contributions from all quasiharmonic modes; see Computational Methods) together with the associated corrections terms for quasiharmonic mode anharmonicity ( $\Delta S_{\text{cl}}^{\text{ah}}$ ) and mode (pairwise supralinear) correlation ( $\Delta S_{\text{cl}}^{\text{pc}}$ ) are reported in Table 2 for the W191G cavity and gating-loop regions for the three MD trajectories. The  $E_{\text{cl}}^{\text{pot}}$ ,  $E_{\text{cl}}^{\text{coval}}$ , and  $E_{\text{cl}}^{\text{nb}}$  terms are fully converged (not shown) and qualitatively<sup>[27]</sup> account for corresponding enthalpy contributions. The  $\Delta S_{\text{cl}}^{\text{ah}}$  corrections are negative and small overall (at most 0.5% of  $S_{\text{qm}}^{\text{h}}$ ), which agrees with previous results in the context of small flexible molecules of diverse chemical nature.<sup>[36,43–45]</sup> The corrections  $\Delta S_{\text{cl}}^{\text{pc}}$  are also negative, but of significantly larger relative magnitude (27–73% of  $S_{\text{qm}}^{\text{h}}$ ). Interestingly,  $\Delta S_{\text{cl}}^{\text{pc}}$  correction terms can be directly related to the motional correlations of the W191G cavity and gating-loop regions. We observe larger relative magnitudes for the W191G cavity than the gating-loop regions (**ref**: 43 vs 30%; **bb**: 73 vs 41%; **open**: 43 vs 27%) and considerably higher correlation effects for the **bb** simulation.

The correction terms we estimated are far from being negligible, of significantly different magnitude in all thermodynamic states considered, and omitting these terms would lead to 1) significant overestimation of the absolute single-molecule configurational entropy, and 2) inaccurate estimates of the difference between the thermodynamic states of interest. These general methodological observations are in line with those reported for reversible peptide folding.<sup>[36]</sup>

## 2.3. Entropic Effects on the Receptor Free Energy

The corrected entropy values  $S^{\text{ctd}}$  elucidate the link between receptor dynamics, flexibility, and thermodynamics (see Table 2). A significant decrease of  $S^{\text{ctd}}$  can be observed for the W191G cavity upon binding of 2a5mt (**ref**: 1153; **bb**: 466; **open**: 1175 J K $^{-1}$  mol $^{-1}$ ). This mainly follows from a substantially larger motional correlation in the W191G–2a5mt complex, as demonstrated by comparison between  $S^{\text{ctd}}$  and  $S_{\text{qm}}^{\text{h}}$  values (**ref**: 2044; **bb**: 1736; **open**: 2078 J K $^{-1}$  mol $^{-1}$ ). In the bound state **bb**, a significant contribution to the high motional correlation in the W191G cavity is the restriction to one energy well of Met230 side-chain sampling. A pronounced reduction of gating-loop entropy occurs upon W191G–2a5mt binding, while a sizeable increase can be observed upon opening of the gate (**ref**: 601; **bb**: 484; **open**: 726 J K $^{-1}$  mol $^{-1}$ ). Our results agree with higher experimental *B*-factors<sup>[10]</sup> and an increased conformational diversity for the open versus closed gating loop.<sup>[14]</sup>

Once a change in entropy is calculated, the resulting effect on the solute-only free energy ( $-T \cdot \Delta S^{\text{ctd}}$ ; W191G cavity or gating loop) can be estimated.<sup>[18,19]</sup> Taking the **ref** simulation as the reference thermodynamic state at 300 K, the cavity flexibility destabilizes the W191G–2a5mt complex by 206 kJ mol $^{-1}$ . The combined effects of releasing the K $^{+}$  ion and opening the gating loop increase the stability of W191G by 7 kJ mol $^{-1}$ . Similarly, decreasing the gating-loop flexibility destabilizes the



**Table 2.** Estimated single-molecule energetic contributions, quasiharmonic entropies, corresponding correction terms, and receptor flexibility contributions to changes in free energy.<sup>[a]</sup>

| Protein region | MD ensemble | $E_{\text{cl}}^{\text{pot}}$ | $E_{\text{cl}}^{\text{coval}}$ | $E_{\text{cl}}^{\text{nb}}$ | $S_{\text{qm}}^{\text{h}}$ | $\Delta S_{\text{cl}}^{\text{ah}}$    | $\Delta S_{\text{cl}}^{\text{pc}}$ | $S^{\text{ctd}}$ | $-T \cdot \Delta S^{\text{ctd}}$ |
|----------------|-------------|------------------------------|--------------------------------|-----------------------------|----------------------------|---------------------------------------|------------------------------------|------------------|----------------------------------|
|                |             |                              | [kJ mol <sup>-1</sup> ]        |                             |                            | [JK <sup>-1</sup> mol <sup>-1</sup> ] |                                    |                  | [kJ mol <sup>-1</sup> ]          |
| W191G cavity   | <b>ref</b>  | -900                         | 83                             | -983                        | 2044                       | -6 (0.3)                              | -885 (43)                          | 1153             | 0                                |
|                | <b>bb</b>   | -1178                        | 80                             | -1258                       | 1736                       | -7 (0.4)                              | -1263 (73)                         | 466              | 206                              |
|                | <b>open</b> | -954                         | 72                             | -1026                       | 2078                       | -5 (0.5)                              | -898 (43)                          | 1175             | -7                               |
| Gating loop    | <b>ref</b>  | -343                         | 72                             | -415                        | 862                        | -3 (0.3)                              | -258 (30)                          | 601              | 0                                |
|                | <b>bb</b>   | -378                         | 75                             | -453                        | 822                        | -3 (0.4)                              | -335 (41)                          | 484              | 110                              |
|                | <b>open</b> | -408                         | 80                             | -328                        | 1002                       | -3 (0.3)                              | -273 (27)                          | 726              | -37                              |

[a] The energetic contributions (evaluated with the classical MD force field) are the ensemble-averaged values. The upper bound of the quasiharmonic entropies  $S_{\text{qm}}^{\text{h}}$  (evaluated by using the quantum-mechanical formula for the entropy of a harmonic oscillator) are reported together with their (classically derived) corrections for mode anharmonicity ( $\Delta S_{\text{cl}}^{\text{ah}}$ ) and (pairwise supralinear) correlations ( $\Delta S_{\text{cl}}^{\text{pc}}$ ), leading to the corrected values  $S^{\text{ctd}} = S_{\text{qm}}^{\text{h}} + \Delta S_{\text{cl}}^{\text{ah}} + \Delta S_{\text{cl}}^{\text{pc}}$ . The quantity  $-T \cdot \Delta S^{\text{ctd}}$ , where  $T$  is the temperature (300 K) and  $\Delta S^{\text{ctd}}$  the differences in  $S^{\text{ctd}}$  for a given region, is also reported as an indication of the corresponding free-energy contribution (relative to **ref**) due to changes in cavity or gating-loop flexibility. Relative values of the entropy corrections (in percent with respect to  $S_{\text{qm}}^{\text{h}}$ ) are reported between parentheses. The ensemble codes refer to Table 1.

W191G–2a5mt complex by 110 kJ mol<sup>-1</sup>, but increased flexibility increases the stability of W191G by 37 kJ mol<sup>-1</sup> when opening the gating loop and releasing the K<sup>+</sup> ion. A change of (overall solute and solvent) molecular entropy<sup>[20,35]</sup> upon binding 2a5mt of about 30 kJ mol<sup>-1</sup> was measured.<sup>[12]</sup> Therefore, the solute–solute component of the overall molecular entropy terms must be overcompensated by favorable solute–solvent and solvent–solvent effects. This latter hypothesis is also supported by the ordering effect on cavity water dynamics due to the K<sup>+</sup> ion in the W191G cavity,<sup>[14]</sup> which suggests a large and favorable solvent–solvent (reorganization) entropy change upon K<sup>+</sup> displacement and cavity desolvation. Changes upon binding of (overall system) free energy (in the range -30 to -16 kJ mol<sup>-1</sup>), enthalpy (in the range -96 to -17 kJ mol<sup>-1</sup>), and molecular entropy (in the range -230 to 17 JK<sup>-1</sup> mol<sup>-1</sup>) have been measured<sup>[12]</sup> for thirteen ligands and are fully compatible with the receptor-entropy changes described in this work.

We note that the numerical accuracy of the absolute entropies and their differences reported in this work depend, as for any simulation study, on 1) the quality of the theory and model, 2) the accuracy of the force field, 3) the degree of sampling, statistics, and convergence reached in the simulations, 4) the quality of the simulation software, and 5) how competently the simulation software is used. Concerning point (1) we employed standard equilibrium statistical mechanics<sup>[36]</sup> and an atomic-level explicit-solvent MD simulation model. Concerning limitation (2), we made use of the highly accurate GROMOS force field, the parametrization of which explicitly includes hydration thermodynamics.<sup>[39]</sup> Concerning limitation (3), we reported in the text a quantitative analysis of convergence. A more extensive sampling of the same W191G thermodynamic states will certainly increase the accuracy of these results and should confirm the major findings of this work. In fact, it is reasonable to imagine that the thermodynamic state mainly affected by the sampling problem is the **open** one (see Table 2), which corresponds to a more flexible receptor state. Longer MD runs and future entropy calculations will likely reveal even larger  $-T \cdot \Delta S^{\text{ctd}}$  contributions for the binding process investigated. Concerning points (4) and (5), the reader is referred to

the Computational Methods, which allows complete reproduction of the results presented herein.

### 3. Conclusions

We conclude that the flexibility of W191G plays a crucial role in both dynamic and thermodynamic changes upon binding 2a5mt, which reflects the closed/open states of its gating loop. We quantified the sizeable single-molecule configurational entropy loss, dominated by motional correlation effects, that occurs upon binding for both the W191G cavity and gating-loop regions. A larger entropy characterizes the 190–195 gating loop in its open versus closed ensemble. Receptor flexibility accounts for a significant part of the compensating entropy/enthalpy terms of the binding free energy. These effects are key determinants of (bio)molecular association in general, and computational methodologies will benefit from their inclusion, in terms of predictive power and transferability. The results presented can be used to complement experimental measurements with single-molecule thermodynamic data.

We stress that the findings presented here are a lower-bound case in the general context of receptor entropy in protein–ligand binding. In other words, in the W191G system the changes upon binding of conformational sampling, single-molecule configurational entropy, and motional correlations are limited to the binding cavity and the 190–195 gating loop regions. For macromolecular receptors, in general, these changes may be expected to be of even larger magnitude when allosteric effects or large conformational rearrangements accompany the binding process. Therefore, this latter consideration additionally supports the major finding of our work, that is, that the entropic impact of receptor flexibility is a sizeable and generally underestimated component of biomolecular association thermodynamics.

Three other major conclusions are apparent from our study.

First, it is misleading to interpret ligand-binding thermodynamics on the basis of rigid receptor structures. Estimates of binding affinities based on single time/ensemble-averaged receptor structures (e.g. rigid-receptor docking or single-point ab initio calculations based on X-ray protein models, i.e. zero-re-

ceptor entropy calculations) are likely—in the best case—to be only fortuitously correct due to error cancellation of the corresponding enthalpy and entropy terms involved. In fact, we have shown that even local flexibility effects, such as the side chain wiggling of cavity residues, have a large entropic impact on the overall free energy.

Second, the computational methodology employed in this work, based on the anharmonicity and correlation correction terms estimated through a complete quasiharmonic analysis, is a robust and accurate tool for estimating configurational entropies from computer simulations of molecular systems. Provided that these correction terms are taken into account, the quasiharmonic approximation can be successfully applied also to macromolecular systems characterized by multiple-well free-energy surfaces.

Third, after validation with available experimental data, accurate explicit-solvent MD simulations can provide (thermo)dynamic insight at the molecular level otherwise inaccessible to experiments.

## Computational Methods

**Molecular Dynamics Simulations:** Three MD trajectories of the W191G cavity mutant of cytochrome c peroxidase from *E. coli* (W191G; 290 residues) in explicit water at 300 K (**ref**: initial apo closed-gate W191G coordinates from PDB 1AA4; **bb**: initial closed-gate W191G–2a5mt complex coordinates from PDB 1AEN; **open**: initial W191G apo open-gate coordinates based on PDB 1RYC after deleting bzi) were generated using the GROMOS05 software,<sup>[46]</sup> the GROMOS 45 A4 force field,<sup>[47,48]</sup> and compatible K<sup>+</sup> ion parameters<sup>[49]</sup> and SPC water model.<sup>[50]</sup> For setup of the systems see Table 1. Methodological details and comparison to experiment for initial 10 ns MD periods after equilibration have been previously reported.<sup>[14]</sup> This work is based on extended 50 ns equilibrated trajectories conveniently obtained using a fast grid-based pairlist-construction algorithm (cell-mask edge 0.4 nm; atomic-level cutoff).<sup>[51]</sup> The observations reported on the stability of the first 10 ns of these trajectories still hold for the 50 ns trajectories used here. Trajectory snapshots were extracted every 1 ps along each of the three equilibrated 50 ns MD trajectories and used for analysis.

**Definition of the Cavity and Loop Regions:** The cavity region includes His 175, Leu 177, Lys 179, Thr 180, Pro 190, Asn 195, Phe 202, Met 230, Met 231, Leu 232, and Asp 235. The loop region includes Pro 190, Gly 191, Gly 192, Ala 193, Ala 194, and Asn 195.<sup>[14]</sup>  $\chi$  dihedral sampling for Thr 180, Pro 190, and Phe 202 displays no barrier crossing and systematically overlaps with the experimental values from X-ray crystal structures (not shown).

**Dihedral Transitions:** Monitoring of torsional dihedral angle transitions was performed as defined in ref. [47]. This procedure delivers all transitions that have occurred since the start of the 50 ns simulation period, including only those transition events involving the sampling of a neighboring energy well, but excluding events of barrier crossing only. The average time between two transitions ( $t_{\text{trans}}$ ) was estimated as the total simulation time divided by the number of transition events.

**Configurational Entropy Calculations:** Single-molecule<sup>[35]</sup> (absolute) configurational entropies were estimated on the basis of a complete quasiharmonic analysis,<sup>[36]</sup> using all atoms of the cavity (68 atoms, 198 matrix diagonal elements) or the 190–195 loop (37

atoms, 105 matrix diagonal elements) region, after removing their overall translation and rotation.<sup>[52]</sup> The quasiharmonic entropy upper-bound estimate ( $S_{\text{qm}}^{\text{h}}$ ) and its corrections for anharmonicities in the quasiharmonic modes ( $\Delta S_{\text{cl}}^{\text{ah}}$ ) and for (supralinear) pairwise correlations among the modes ( $\Delta S_{\text{cl}}^{\text{pc}}$ ) were evaluated at the classical level. The underlying theory, assumptions, approximations, and practical implementation are described elsewhere,<sup>[36]</sup> as are previous applications.<sup>[36,43–45]</sup> For each thermodynamic state of interest, numerical integration for both  $\Delta S_{\text{cl}}^{\text{ah}}$  and  $\Delta S_{\text{cl}}^{\text{pc}}$  corrections was performed with a range of seven alternative integration bin sizes to estimate the optimal (1D or 2D) integral value, as described elsewhere.<sup>[36]</sup> Thus, the anharmonicity correction  $\Delta S_{\text{cl}}^{\text{ah}}$  involved the calculation of (cavity:  $3 \times 1386$ ; loop:  $3 \times 735$ ) 1D integrals throughout the  $5 \times 10^4$  projections onto trajectory structures. The pairwise (supralinear) correlation correction  $\Delta S_{\text{cl}}^{\text{pc}}$  was calculated numerically by summing the corresponding contributions over all (unique) pairs of modes, totaling (cavity:  $3 \times 136\,521$ ; loop:  $3 \times 38\,220$ ) 2D integrals throughout the  $5 \times 10^4$  projections onto trajectory structures. Corrections  $\Delta S_{\text{cl}}^{\text{ah}}$  and  $\Delta S_{\text{cl}}^{\text{pc}}$  are additive and lead to the corrected single-molecule quasiharmonic entropy estimates  $S^{\text{std}}$  used for discussion.

The numerical error of the final  $S_{\text{qm}}^{\text{h}}$  values was evaluated after block averaging of ten 5 ns subensembles of structures. This analysis shows that the average error over all simulations is about  $11 \text{ JK}^{-1} \text{ mol}^{-1}$  with a maximum of about  $16 \text{ JK}^{-1} \text{ mol}^{-1}$  observed for the gating loop of the **open** ensemble.

We note that calculating quasiharmonic mode correlations of higher order than the pairwise supralinear correlations explicitly taken into account in this work is currently computationally prohibitive due to finite sampling limitations and to their poor numerical accuracy. However, higher order correlations, even if intrinsically smaller, may still be significant because they are more numerous.<sup>[36]</sup>

## Acknowledgements

R.B. warmly thanks Veronica Nieves and Alemayehu Gorfe for critically reading the manuscript. The Center for Theoretical Biological Physics is acknowledged for the computing resources employed. This work has been funded, in part, by the National Science Foundation, the Howard Hughes Medical Institute, and the National Institute of Health. Additional support has been provided by the National Biomedical Computation Resource and Acceleris Inc.

**Keywords:** molecular dynamics • proteins • quasiharmonic analysis • receptors • thermodynamics

- [1] P. M. Dean, *Molecular Foundations of Drug-Receptor Interaction*, Cambridge University Press, Cambridge, 1987.
- [2] D. E. Koshland, Jr., *Angew. Chem.* 1994, 106, 2468–2472; *Angew. Chem. Int. Ed. Engl.* 1994, 33, 2375–2378.
- [3] E. di Cera, *Thermodynamic Theory of Site-Specific Binding Processes in Biological Macromolecules*, Cambridge University Press, Cambridge, 1995.
- [4] H.-J. Böhm, G. Klebe, *Angew. Chem.* 1996, 108, 2750–2778; *Angew. Chem. Int. Ed. Engl.* 1996, 35, 2588–2614.
- [5] A. M. Davis, S. J. Teague, *Angew. Chem.* 1999, 111, 778–792; *Angew. Chem. Int. Ed.* 1999, 38, 736–749.
- [6] *Drug-Receptor Thermodynamics: Introduction and Applications* (Ed.: R. B. Raffa), Wiley, New York, 2001.

- [7] H. Gohlke, G. Klebe, *Angew. Chem.* **2002**, *114*, 2764–2798; *Angew. Chem. Int. Ed.* **2002**, *41*, 2644–2676.
- [8] W. L. Jorgensen, *Science* **2004**, *303*, 1813–1818.
- [9] M. M. Fitzgerald, M. L. Trester, G. M. Jensen, D. E. McRee, D. B. Goodin, *Protein Sci.* **1995**, *4*, 1844–1850.
- [10] M. M. Fitzgerald, R. A. Musah, D. E. McRee, D. B. Goodin, *Nat. Struct. Biol.* **1996**, *3*, 626–631.
- [11] R. A. Musah, D. B. Goodin, *Biochemistry* **1997**, *36*, 11665–11674.
- [12] R. A. Musah, G. M. Jensen, S. W. Bunte, R. J. Rosenfeld, D. B. Goodin, *J. Mol. Biol.* **2002**, *315*, 845–857.
- [13] R. Brenk, S. W. Vetter, S. E. Boyce, D. B. Goodin, B. K. Shoichet, *J. Mol. Biol.* **2006**, *357*, 1449–1470.
- [14] R. Baron, J. A. McCammon, *Biochemistry* **2007**, *46*, 10629–10642.
- [15] H. R. Bosshard, *News Physiol. Sci.* **2001**, *16*, 171–173.
- [16] H. A. Carlson, *Curr. Opin. Chem. Biol.* **2002**, *6*, 447–452.
- [17] J. R. Schames, R. H. Henchman, J. S. Siegel, C. A. Sottriffer, H. Ni, J. A. McCammon, *J. Med. Chem.* **2004**, *47*, 1879–1881.
- [18] E. Fermi, *Thermodynamics*, Dover, New York, **1936**.
- [19] F. Reif, *Fundamentals of Statistical and Thermal Physics*, McGraw-Hill, Singapore, **1985**.
- [20] In this work usage of the terms “flexibility”, “dynamics”, “thermodynamics”, “single-molecule”, and “molecular” is based on their statistical mechanics definitions. Dynamics is related to phase-space sampling. Thermodynamics concerns the sampled configurational space only, that is, configurations not momenta (see refs. [18,19]). For example, different dynamics, due to different degrees of freedom momenta and frequencies, may still correspond to identical thermodynamic properties. Flexibility involves both aspects and generally refers to ensemble average properties only (e.g. mean-square fluctuations of a molecular system). For a definition of single-molecule and molecular entropy terms see ref. [35].
- [21] M. Akke, R. Brüschweiler, A. G. Palmer III, *J. Am. Chem. Soc.* **1993**, *115*, 9832–9833.
- [22] A. Cooper, *Curr. Opin. Chem. Biol.* **1999**, *3*, 557–563.
- [23] J. D. Forman-Kay, *Nat. Struct. Biol.* **1999**, *6*, 1086–1087.
- [24] M. J. Stone, *Acc. Chem. Res.* **2001**, *34*, 379–388.
- [25] S. W. Homans, *ChemBioChem* **2005**, *6*, 1585–1591.
- [26] K. K. Frederick, M. S. Marlow, K. G. Valentine, A. J. Wand, *Nature* **2007**, *448*, 325–329.
- [27] A. E. Mark, W. F. van Gunsteren, *J. Mol. Biol.* **1994**, *240*, 167–176.
- [28] M. K. Gilson, J. A. Given, B. L. Bush, J. A. McCammon, *Biophys. J.* **1997**, *72*, 1047–1069.
- [29] W. P. Reinhardt, M. A. Miller, L. M. Amon, *Acc. Chem. Res.* **2001**, *34*, 607–614.
- [30] C. Peter, C. Oostenbrink, A. van Dorp, W. F. van Gunsteren, *J. Chem. Phys.* **2004**, *120*, 2652–2661.
- [31] J. M. Swanson, R. H. Henchman, J. A. McCammon, *Biophys. J.* **2004**, *86*, 67–74.
- [32] J. A. McCammon, *Biochim. Biophys. Acta.* **2005**, *1754*, 221–224.
- [33] J. Carlsson, J. Åqvist, *J. Phys. Chem. B* **2005**, *109*, 6448–6456.
- [34] J. Carlsson, J. Åqvist, *Phys. Chem. Chem. Phys.* **2006**, *8*, 5385–5395.
- [35] R. Baron, A. H. de Vries, P. H. Hünenberger, W. F. van Gunsteren, *J. Phys. Chem. B* **2006**, *110*, 8464–8473.
- [36] R. Baron, W. F. van Gunsteren, P. H. Hünenberger, *Trends Phys. Chem.* **2006**, *11*, 87–122.
- [37] R. Baron, D. Trzesniak, A. H. de Vries, A. Elsener, S. J. Marrink, W. F. van Gunsteren, *ChemPhysChem* **2007**, *8*, 452–461.
- [38] C. E. Chang, W. Chen, M. K. Gilson, *Proc. Natl. Acad. Sci. USA* **2007**, *104*, 1534–1539.
- [39] W. F. van Gunsteren, D. Bakowies, R. Baron, I. Chandrasekhar, M. Christen, X. Daura, P. Gee, D. P. Geerke, A. Glättli, P. H. Hünenberger, M. A. Kastenholz, C. Oostenbrink, M. Schenk, D. Trzesniak, N. F. van der Vegt, H. B. Yu, *Angew. Chem.* **2006**, *118*, 4168–4198; *Angew. Chem. Int. Ed.* **2006**, *45*, 4064–4092.
- [40] D. Bakowies, W. F. van Gunsteren, *J. Mol. Biol.* **2002**, *315*, 713–736.
- [41] S. Salaniwal, E. S. Manas, J. C. Alvarez, R. J. Unwalla, *Proteins* **2007**, *66*, 422–435.
- [42] A. M. Ruvinsky, *J. Comput. Chem.* **2007**, *28*, 1364–1372.
- [43] C. S. Pereira, D. Kony, R. Baron, M. Müller, W. F. van Gunsteren, P. H. Hünenberger, *Biophys. J.* **2006**, *90*, 4337–4344.
- [44] R. Baron, A. H. de Vries, P. H. Hünenberger, W. F. van Gunsteren, *J. Phys. Chem. B* **2006**, *110*, 15602–15614.
- [45] C. S. Pereira, D. Kony, R. Baron, M. Müller, W. F. van Gunsteren, P. H. Hünenberger, *Biophys. J.* **2007**, *93*, 704–707.
- [46] M. Christen, P. H. Hünenberger, D. Bakowies, R. Baron, R. Bürgi, D. P. Geerke, T. N. Heinz, M. A. Kastenholz, V. Kräutler, C. Oostenbrink, C. Peter, D. Trzesniak, W. F. van Gunsteren, *J. Comput. Chem.* **2005**, *26*, 1719–1751.
- [47] W. F. van Gunsteren, S. R. Billeter, A. A. Eising, P. H. Hünenberger, P. Krüger, A. E. Mark, W. R. P. Scott, I. G. Tironi, *Biomolecular Simulation: The GROMOS96 Manual and User Guide*, vdf Hochschulverlag AG an der ETH Zurich/BIOMOS b.v. Groningen, Zurich/Groningen, **1996**.
- [48] T. A. Soares, P. H. Hünenberger, M. A. Kastenholz, V. Kräutler, T. Lenz, R. D. Lins, C. Oostenbrink, W. F. Van Gunsteren, *J. Comput. Chem.* **2005**, *26*, 725–737.
- [49] J. Åqvist, *J. Phys. Chem.* **1990**, *94*, 8021–8024.
- [50] H. J. C. Berendsen, *Interaction Models for Water in Relation to Protein Hydration* (Ed.: B. E. Pullman), Reidel, Dordrecht, **1981**.
- [51] T. N. Heinz, P. H. Hünenberger, *J. Comput. Chem.* **2004**, *25*, 1474–1486.
- [52] A. D. McLachlan, *J. Mol. Biol.* **1979**, *128*, 49–79.

Received: December 22, 2007  
Published online on April 16, 2008